Original paper

Zalužany – a circular structure in the Czech Republic accompanied by glass of granodiorite composition

Stanislav VRÁNA[1†], Jan MRLINA[2*], Radek ŠKODA[3], Patricie HALODOVÁ[1]

[1] *Czech Geological Survey, Klárov 3, 118 21 Prague 1, Czech Republic*
[2] *Institute of Geophysics, Czech Academy of Sciences, Boční II/1401, 141 00 Prague 4, Czech Republic; jan@ig.cas.cz*
[3] *Department of Geological Sciences, Masaryk University, Kotlářská 2, 611 37 Brno, Czech Republic*
[*] *Corresponding author*
[†] *Deceased*

The Hejný Pond, 500 × 400 m, southeast of the Zalužany village in central Bohemia, attracted attention as a possible impact structure. The pond has a notable bilateral symmetry with an axis oriented NW–SE, indicating a significant subhorizontal vector in the overall deformation pattern. A negative gravity anomaly elongated in the same direction (600 × 300 m) with the amplitude of –0.35 mGal was disclosed by detailed gravity survey. The incomplete ring of elevations suggests slightly uplifted basement segments with a diameter of 1 km. Search for glass and other possible indicators of shock metamorphism resulted in a find of glass fragments 22 to 37 mm across. The glass has composition comparable to the local Kozárovice hornblende–biotite granodiorite of the Central Bohemian Plutonic Complex. Unusual features include locally high contamination by iron (up to 10–13 wt. % FeOt) and abundant cristobalite. The absence of planar deformation features in quartz and feldspars together with the absence of platinum-group elements and Ni enrichment in local glass may be considered as obstacles in defining Zalužany as an impact structure. Although glass fragments are rare at the locality, and the considerable Quaternary erosion, the occurrence of rock inclusions in two of the fragments makes the Zalužany structure a promising object for future study.

Keywords: circular structure, gravimetry, Central Bohemian Pluton, glass
Received: 10 November 2017; accepted: 12 April 2019; handling editor: R. Skála
The online version of this article (doi: 10.3190/jgeosci.281) contains supplementary electronic material.

1. Introduction

The last decades in study of impact structures have brought evidence that meteorite impact events are an important geological process. Attention was mainly focused on large structures with d = 10–100 km, often of rather ancient age. These large impact structures serve as the most important examples of changing the morphology of planet surface and carry reserves of economically important materials (Reimold et al. 2005).

Small meteorite craters and impact structures with d = 0.2–2 km feature major problems of preservation owing to erosion over prolonged periods. Even a moderate progress in erosion is likely to render such structures as unrecognizable relicts. Owing to this situation, recognized small structures are dominantly of young age. Additional aspect of the small and young structures is their relation to the Near Earth Object Program, which deals with the present and near future risk of impact on our planet (*https://cneos.jpl.nasa.gov/sentry*, *https://www.nasa.gov/planetarydefense/overview*).

However, the circular structures can be also of volcanic origin. For instance, in Western Bohemia, along the border of the Czech Republic with Germany, circular volcanic structures occur in the area of recent seismicity and upper mantle fluid debouches. The youngest, in terms of discovery date, the Quaternary Mýtina maar/diatreme near Cheb (Ohře/Eger rift) is *c.* 0.5 km in diameter (Mrlina et al. 2009). The circular depression is of Mid-Pleistocene age (0.288 Ma according to Mrlina et al. 2007). This structure and related Quaternary forms in that region (Železná hůrka, Komorní hůrka) were produced by alkali basaltic volcanism, represented mainly by volcanic bombs and lapilli, carrying some xenoliths of crystalline rocks derived from the local crystalline basement. This area of young volcanism, some 135 km to the northwest of Zalužany, provides some example that could be used for comparison.

In the current work, we have intended to apply gravity surveying, that had already proven its efficiency in searching for various circular structures (Mrlina et al. 2009; Rohrmüller et al. 2018), in combination with geochemistry and petrology to investigate possible origin of the recently identified Zalužany structure.

2. Geological setting

The Hejný Pond, located 1.5 km SE of the Zalužany village, 70 km south–southwest of Prague, has an elliptical

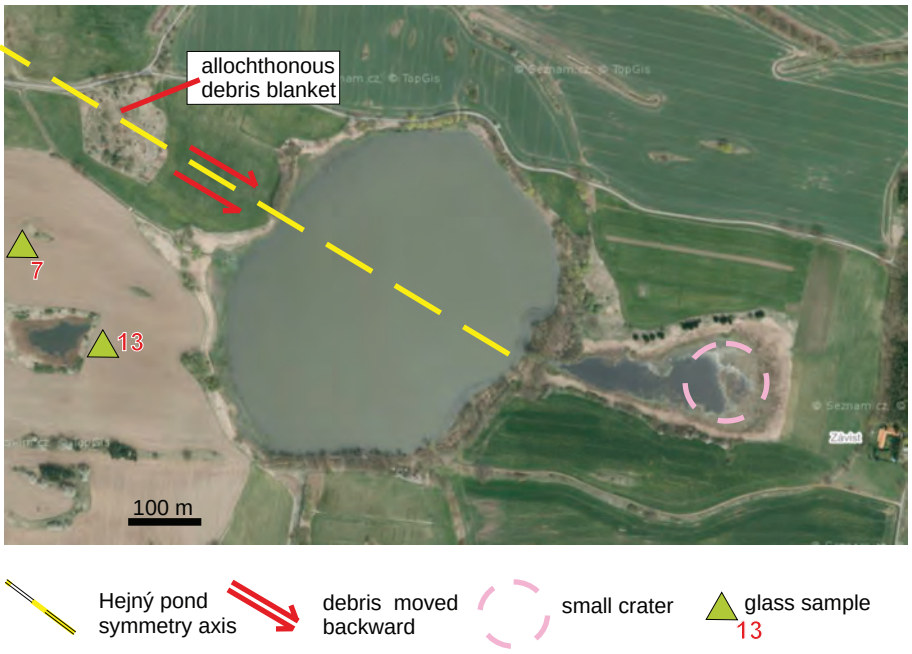

Fig. 1 Shape and bilateral symmetry of the Hejný Pond, including its deviation from a regular circular shape. A small circular structure with diameter of *c.* 100 m occurs 200 m SE of the Hejný Pond. A pivotal allochtonous breccia accumulation (light grey) is seen 150 m NW of the pond. Photo adopted from the Seznam server, *https://mapy.cz*.

shape, 500 × 400 m in diameter (Fig. 1). Several centuries ago a dam was built at the southern side of the original lake. The pond has a strongly defined bi-lateral symmetry, with an axis oriented SE–NW. A single elevation 130 m wide and 150 m long is positioned at the NW periphery of the structure. It is built by displaced material (breccia) (Fig. 1). At the SE foot of the elevation, there is a lower blanket of breccia, gently sloping to the pond, exhibiting an arcuate protrusion into the pond. The morphology suggests a backward transport of material of this protrusion at a late stage. The accumulation can document the importance of the original SE–NW material transport.

The pond is located in a relatively flat area approximately 454 m a.s.l., though an elevated area > 490 m a.s.l. is located just north of the pond (Fig. 2). Low hills, 460 to 466 m a.s.l. at the W, NW and E, make an incomplete ring around the pond, with a diameter of approximately 1 km (Figs 2 and 3a). The incomplete ring of elevations probably represents slightly uplifted basement segments. However, strong erosion resulting from the low erosion base of the Vltava River valley in proximity probably caused removal of at least 10 m thick breccia blanket. The local basement is built by the Kozárovice granodiorite of the Variscan age (Janoušek et al. 2000, 2010). The plutonic body exhibits

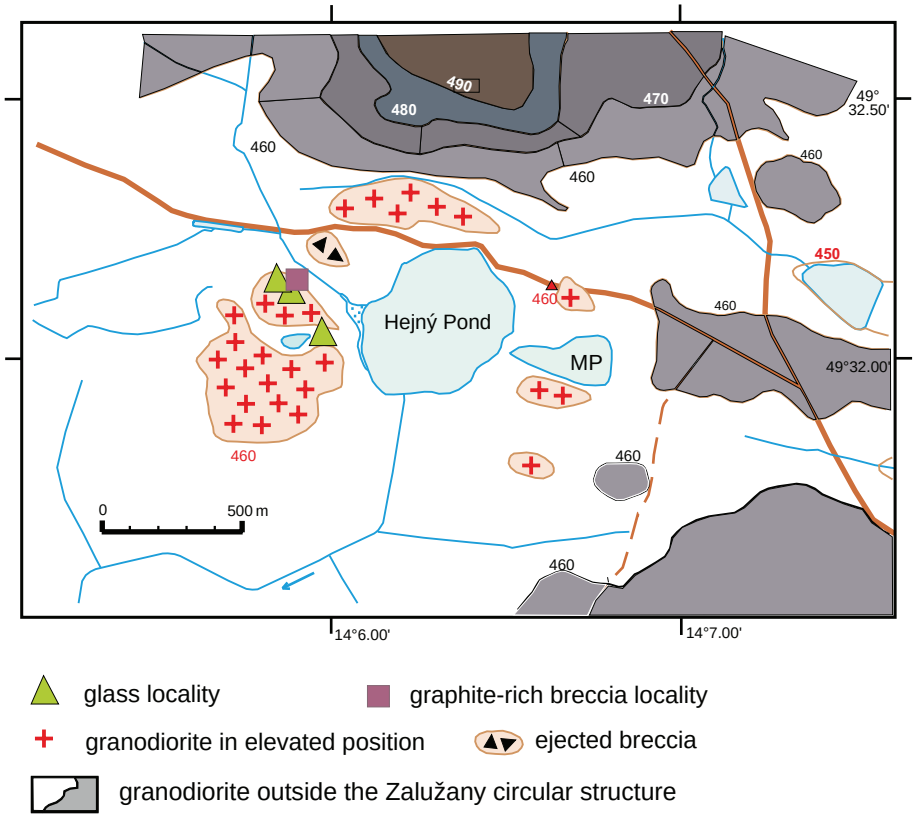

Fig. 2 Simplified topography of the area around the Hejný Pond, 1.5 km southeast of the Zalužany village. The incomplete ring of low hills around the pond, with elevations between 460 and 470 m and *c.* 1 km in diameter is shown in light pink brown with red crosses.

E–W running belts of somewhat variable weathering resistance and hence a slight altitude variation. Some 300 m east of the Hejný Pond is a low marshy depression, *c.* 200 × 100 m in size (Fig. 2, symbol MP). The local Czech name "Na bahnech" translates to "Muddy Place". Erosion results in structureless blankets of granodiorite fragments, blocks and boulders.

3. Methods

3.1. Gravimetry

The gravity survey was performed with the microGal LaCoste&Romberg D-188 gravimeter. The measured data were corrected for instrumental daily drift, height of gravimeter over ground level, change of latitude, Earth tide effects, average rock density in the area (usually 2.67 g/cm^{-3}) and elevation of the observation site. As well, terrain corrections had to be calculated to eliminate the impact of the surrounding relief. The resulting CBA (Complete Bouguer Anomaly) is expressed either in m/s^2 (SI unit), or the widely used mGal (milliGal). The conversion is 1 mGal = 10^{-5} m/s^2. The usual gravimeter resolution is 10^{-7}, or 10^{-8} m/s^2, respectively. The accuracy of measured gravity was 0.006 mGal which is fully sufficient for this kind of survey. The corrected data were then interpolated and presented as a contour map. The regional trend was removed from the map in order to highlight local density variations in the area (Fig. 3b).

3.2. Mineral and rock analyses

Chemical analyses of minerals and glasses were carried out with CAMECA SX 100 WDS electron microprobe

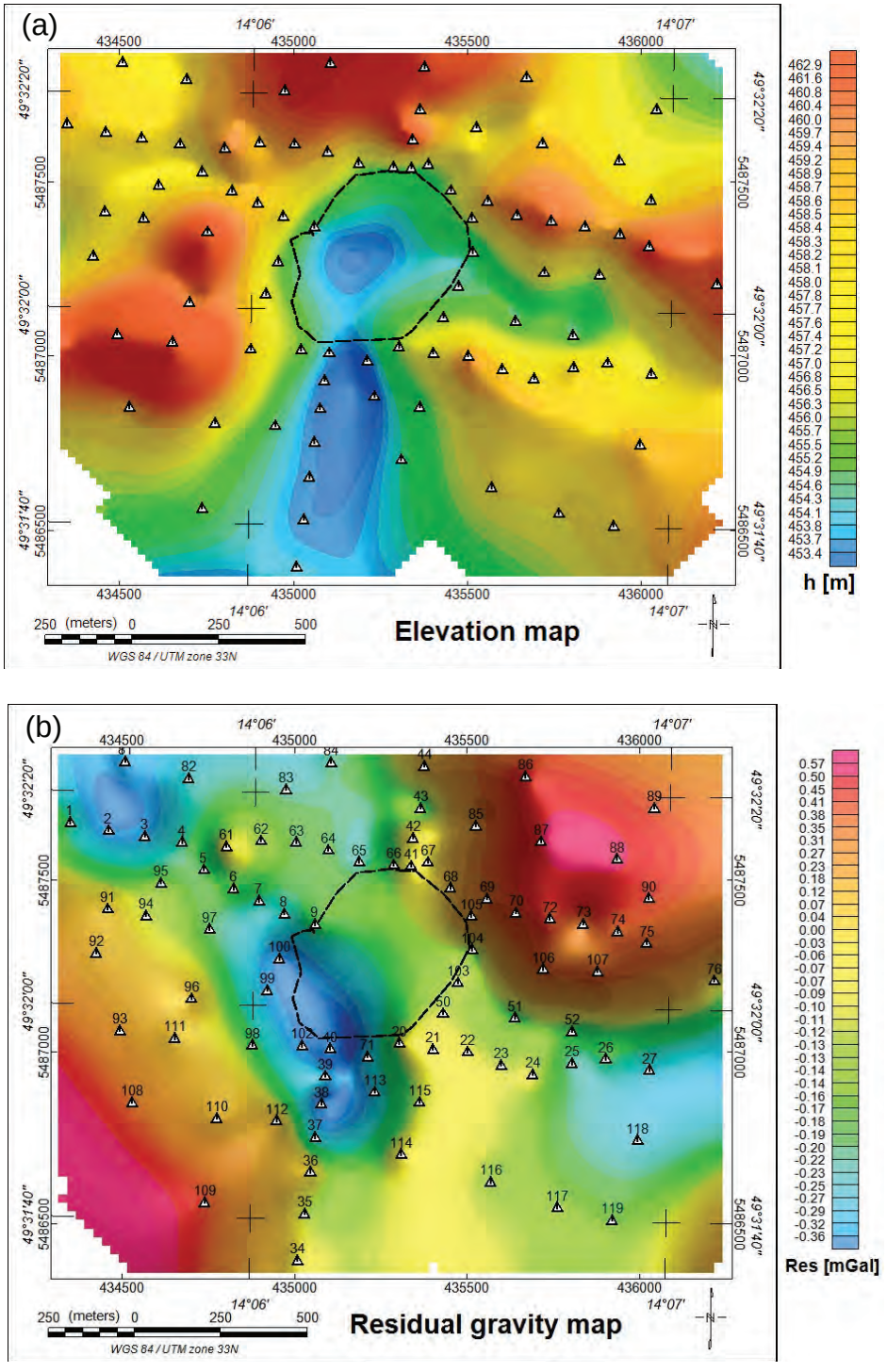

Fig. 3a – Elevation map based on the observed gravity point coordinates only. The valley trending N–S is a drainage outlet from the Hejný Pond. The maximum vertical range is *c.* 10 meters. Broken line marks water edge of the pond. **b** – Residual gravity anomaly map based on 1st order polynomial filtering. Minor edge effects have to be ignored, especially along the eastern border near point 27. The central anomaly close to the pond is clearly highlighted around point 40, as is the minor anomaly to the NW, at around point 2.

(EMP) in the Joint Laboratory of Electron Microscopy and Microanalysis, Department of Geological Sciences, Masaryk University and the Czech Geological Survey, Brno. The analytical conditions varied according to the material analyzed, usually involving 15 kV accelerating voltage, probe current of 10–20 nA and acquisition time of 10–30 s. The standards used for mineral analyses were spessartine (Si, Mn), almandine (Fe), andradite (Ca), $MgAl_2O_4$ (Mg), hornblende (Ti), sanidine (Al, K), albite (Na), fluorapatite (P), chromite (Cr) as well as other minerals containing REE and some minor elements. For glasses, 15 kV accelerating voltage, probe current of 20 nA and beam diameter of 4 μm were employed together with the following standards: albite (Na), sanidine (Si, Al, K), pyrope (Mg), chromite (Cr), vanadinite (Cl), titanite (Ti), wollastonite (Ca), almandine (Fe), spessartine (Mn), topaz (F), Ni_2SiO_4 (Ni) and Co. In either case, the raw data were reduced using PAP matrix corrections (Pouchou and Pichoir 1985). Fine-grained rocks, such as Fe-rich peridotite, were analyzed using Tescan MIRA 3GMU scanning electron microscope housed at the laboratories of the Czech Geological Survey, Prague–Barrandov, fitted with SDD X-MaxN, 80 mm^2 EDS detector and AZtecEnergy AutoPhaseMap software (Oxford Instruments).

Trace-element analyses of the glass NY7 followed the protocol described in detail by Jonášová et al. (2016), which combines decomposition of the sample in HF–HNO_3 mixture followed by dissolution of the residue in 6 M HCl. Trace-element contents in the final diluted solution were measured using an Element 2 ICP-MS housed at the Institute of Geology of the Czech Academy of Sciences. The concentrations of HSE in the same sample were obtained at the same lab using the methods of Jonášová et al. (2016) that include decomposition of the sample in the Carius Tubes (Shirey and Walker 1995) in the reverse aqua regia and presence of ^{185}Re–^{190}Os and ^{191}Ir–^{99}Ru–^{105}Pd–^{194}Pt spikes followed by Os separation by solvent extraction (Cohen and Waters 1996) and Os purification by microdistillation (Birck et al. 1991) and Ir, Ru, Pt, Pd and Re separation by ion-exchange chromatography.

Iridium, Ru, Pd, Pt and Re were measured using an Element 2 coupled with an Aridus II (CETAC) desolvating nebulizer whereas the osmium isotopic compositions were determined by N-TIMS technique (Creaser et al. 1991; Völkening et al. 1991) using a Finnigan MAT 262 mass spectrometer housed at the Czech Geological Survey. Total procedural blanks were <1 pg Re, 0.4 pg Os, 11 pg Ir, 6 pg Ru, 98 pg Pt and 141 pg Pd.

3.3. Raman analysis

Raman analysis of SiO_2 polymorphs (performed on uncoated sample mounts) was done using a Horiba LabRAM HR Evolution spectrometer equipped with Olympus BX-series optical microscope, a diffraction grating with 600 grooves per millimetre, and Peltier-cooled, Si- based charge-coupled device (CCD) detector. Raman spectra were excited with the 633 nm emission of a He–Ne laser (5 mW at the sample surface) and collected in a range of 100–2000 cm^{-1}. With the Olympus 100× objective (NA 0.9) and the system operating in the confocal mode, the lateral resolution was ~1–2 μm^{-1}. Wavenumber calibration was done using the Rayleigh line and Ne-emission lines. The wavenumber accuracy was better than 0.5 cm^{-1}, and the spectral resolution was ~1 cm^{-1}. Maps of Raman spectra were collected at the range of 100–1200 cm^{-1} using 12 mW energy at the sample surface and 3 s dwell time at each pixel. Band fitting was done after appropriate background correction, assuming combined Lorentzian-Gaussian band shapes. Information in Bates (1972) was used in interpretation of the data.

4. Results

4.1. Gravity survey

Considering the location of the circular structure, we performed the survey in two steps. First, we made a reconnaissance survey to determine whether there is any indication of a negative gravity anomaly that could be related to such a structure. Indeed, we found a gravity-low, partly correlating with the Hejný Pond, but the amplitude was relatively small, about –0.35 mGal. Mrlina (2016) showed that rock disintegration of much smaller extent due to karst development, weathering, fracturing, or other geological processes can be recognized by detailed gravity survey. Each gravity point must also be observed for accurate co-ordinates. Consequently, we could propose a simplified model of topography based just on these new data (Fig. 3a).

We decided to perform the second stage of survey in order to cover the area in a semi-regular pattern. Altogether 85 gravity points were measured in the area of about 2.0 × 1.5 km. All the data were then processed to obtain CBA. As the gravity field shows significant horizontal gradient, we consequently performed separation of the regional and residual components of the gravity field to identify the negative anomaly and delineate its extent. We tested a set of polynomial filters and, for simplicity, selected the 1st order filter (Fig. 3b). It turned out that we actually can recognize two negative anomalies – the principal one is related partly to the pond in the centre of the area, and is elliptically extended from here (point 40) to the S and NW, while there is another minor negative indication in the NW of the study area around point

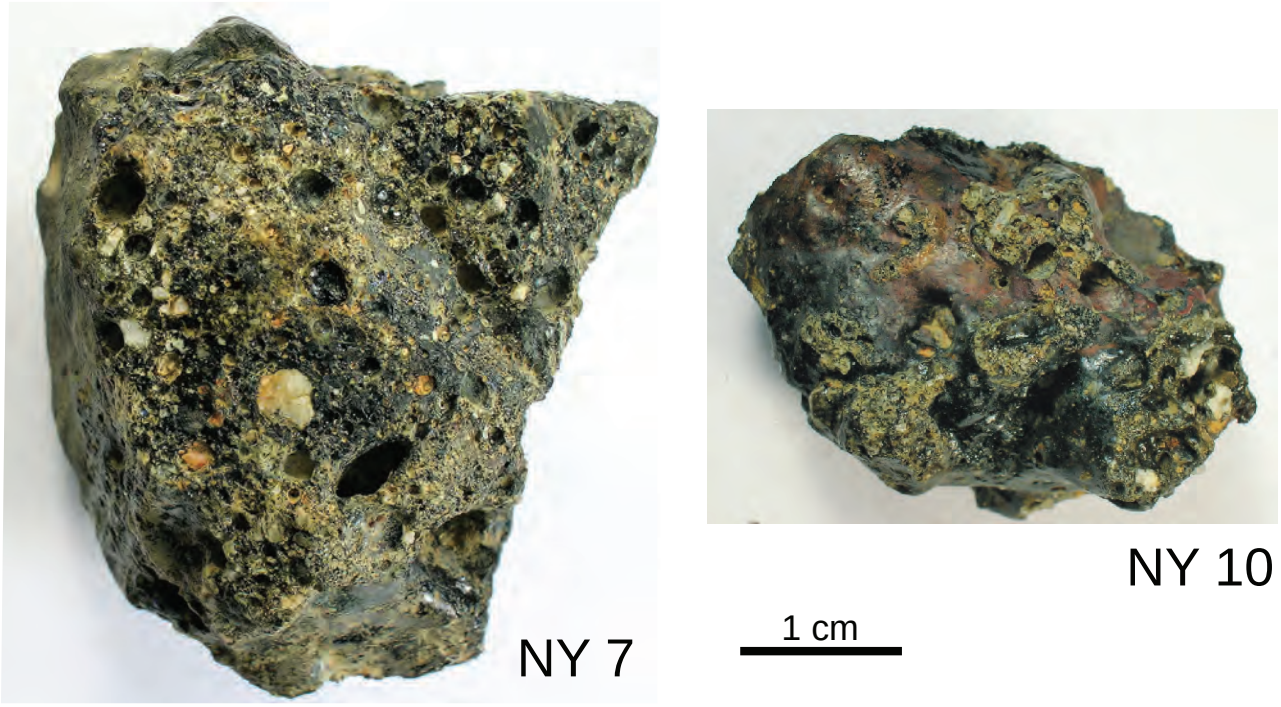

Fig. 4 Glass samples collected in fields 300 m NW of the Hejný Pond.

2. The amplitude of the main anomaly is about –0.35 mGal in relation to the average gravity field in the area; the areal extent is about 1000 × 500 m. In the case of the minor anomaly at NW the amplitude is about –0.30 mGal and the diameter is 200 m.

4.2. Shatter cones and planar deformation features

Shatter cones, together with microscopic planar deformation features, are considered as decisive evidence in support of an impact structure (French and Koeberl 2010). With poor bedrock exposure, search for shatter cones was confined to the blanket of granodiorite fragments mainly west of the structure. At present, shatter cones of a widely acceptable quality or PDFs in quartz are not documented at Zalužany. It is suggested that the situation could be related to erosion.

4.3. The local glass fragments

The glass is relatively rare, with one piece found approximately per two hours. Several pieces collected in the fields (Figs 2, 4) are 22 to 37 mm in size. Colour is brownish grey (Fig. 5). Glass is strongly vesicular with vesicles up to 6 mm across. Inspection with field lens shows numerous angular white tiny inclusions of quartz.

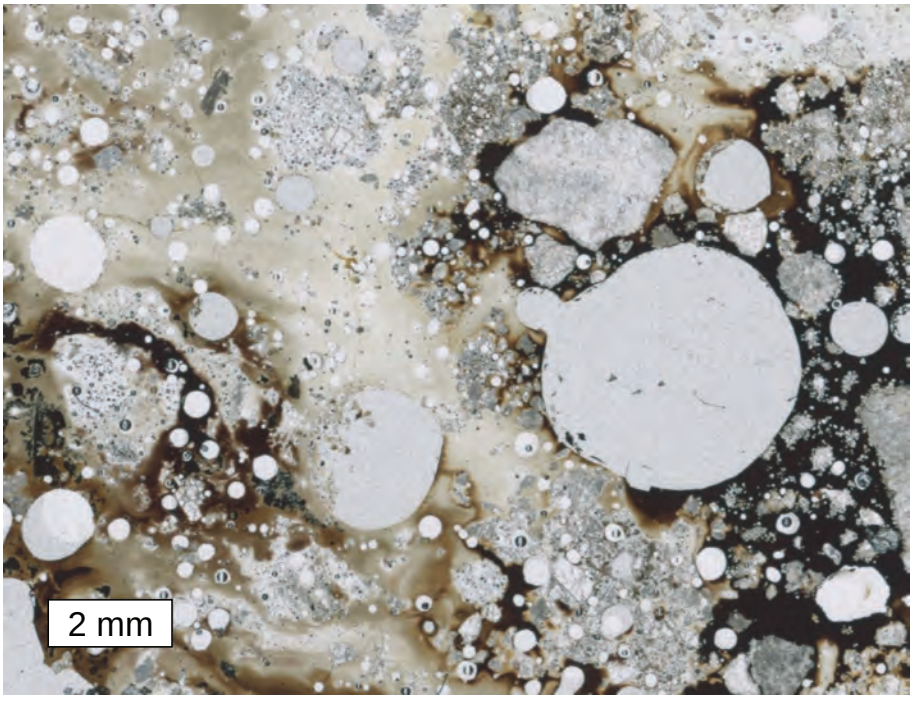

Fig. 5 Structure of glass sample NY13 in thin section. Dark brown domains are rich in Fe. Photomicrograph in transmitted light.

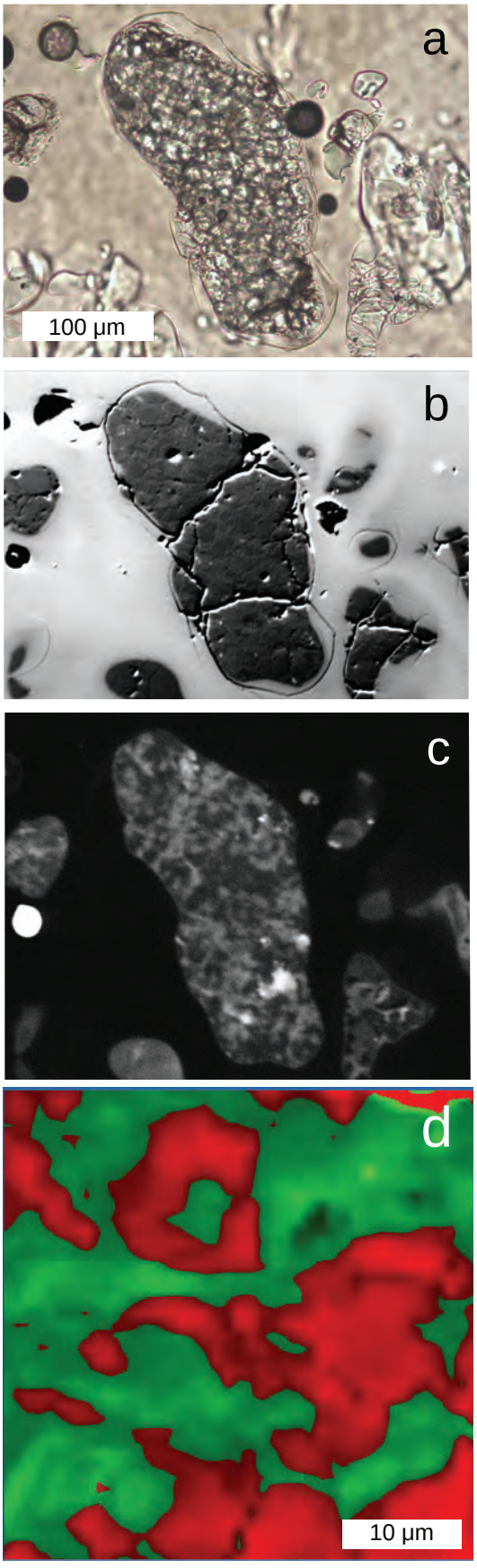

Individual pieces of glass contain variable magnetic properties as the content of magnetite and metallic Fe spherules of microscopic size are variable.

Under the polarizing microscope, glass contains abundant quartz inclusions in quantities from 10 to 30 vol. %. Glass is nearly colourless to dark brown, with strongly defined flow patterns. Quartz clasts in sample NY7 show a variety of patterns of disintegration into subgrains, indicating by optical orientation relative gradual rotation of subgrains by angles of up to 40º. Relatively rarely, quartz grains are free of deformation. At high magnification of electron microscope, quartz clasts show additional complexity. Interior parts of some quartz clasts feature small vesicles, 5 to 30 µm in diameter (Fig. 6). One particular clast was selected for detailed inspection (Fig. 6, sample NY7). Vesicles are seen in a high-contrast BSE image (Fig. 6b). The cathodoluminescence image of this clast indicates a probable presence of at least two different phases. Examination of various parts of the clast with microscopic Raman spectrometry presents evidence that a significant part of the clast has a cristobalite structure but quartz is also present. One particular area 40 µm wide was mapped by Raman spectrometry (Fig. 6d). The resulting map documents nearly equal proportion of cristobalite and quartz. The sample NY7 was examined with Raman spectroscopy for a possible presence of coesite, but none was detected. It is remarkable that no feldspar clasts have been found in the glass and no newly formed feldspar crystallized from glass. The sample NY10 contains one K-rich domain 30 µm long of highly potassic glass corresponding approximately to 70 mol. % of K-feldspar. Such cases should be relatively common, as the dominant target rock – porphyritic hornblende–biotite Kozárovice granodiorite – contains K-feldspar phenocrysts up to 2.5 cm in size.

4.3.1. Coarse cristobalite with ballen structure

Glass sample NY13 contains surprisingly large subhedral crystals up to 60 µm of cristobalite in local dark brown glass, rich in Fe and partly devitrified. Ballen structure, consisting of strongly contoured individual "ballen" 10–20 µm in size, occurs in each cristobalite crystal (Fig. 7). There seems to be no direct quartz precursor and cristobalite probably crystallized from melt. Cristobalite contains 0.46 wt. % FeO and 0.17 wt. % Al_2O_3. The information indicating the role of lechatelierite and

Fig. 6 Quartz clast in glass, with small internal vesicles, altered to quartz–cristobalite aggregate: **a** – Transmitted light microscope image; **b** – High contrast BSE image of the same object; note the small vesicles in the former quartz inclusion; **c** – The same object in a cathodoluminescence image; **d** – Distribution of quartz (red) and cristobalite (green) in the vesiculated granular aggregate, obtained by scanner-mode Raman spectroscopy; contours are smoothed.

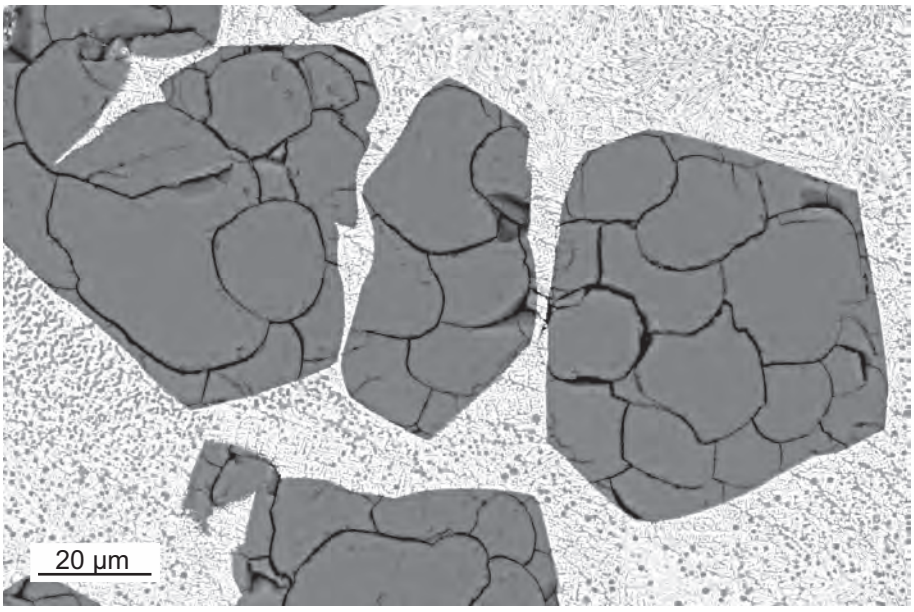

Fig. 7 Back-scattered electron (BSE) image of "ballen" cristobalite in Fe-rich impact glass.

cristobalite in quartz clasts of samples NY7 and NY13 (Figs 8a) and ballen cristobalite in sample NY13 makes this glass rather similar to samples studied by Ferrière et al. (2009).

4.3.2. Reaction of zircon to baddeleyite

The sample NY10 contains number of zircon crystals inherited from source rocks. Some of the crystals show marginal corrosion associated with new formation of ZrO_2, now present as baddeleyite (Fig. 8b). Silica released in the reaction was apparently incorporated in the glass matrix.

4.3.3. Ultramafic Fe-peridotite enclave in vesiculated glass sample NY7

Ultramafic enclave, 15 × 30 mm in size, was found enclosed in vesiculated glass of granodiorite composition (sample NY7). This "Fe-peridotite" is a fine-grained, dark brown rock almost free of vesicles (Figs 9, 10a) that was completely molten probably at the time of inclusion into the vesicular glass. Only about 5 vol. % magnetite and 20–30 % fayalite crystallized and prevailing part solidified as glass (Fig. 10b). Whole-rock composition was obtained by EMP analyses and possible modal composition by Catanorm calculated following Hutchison (1974, implemented by Janoušek et al. 2006) and assuming all

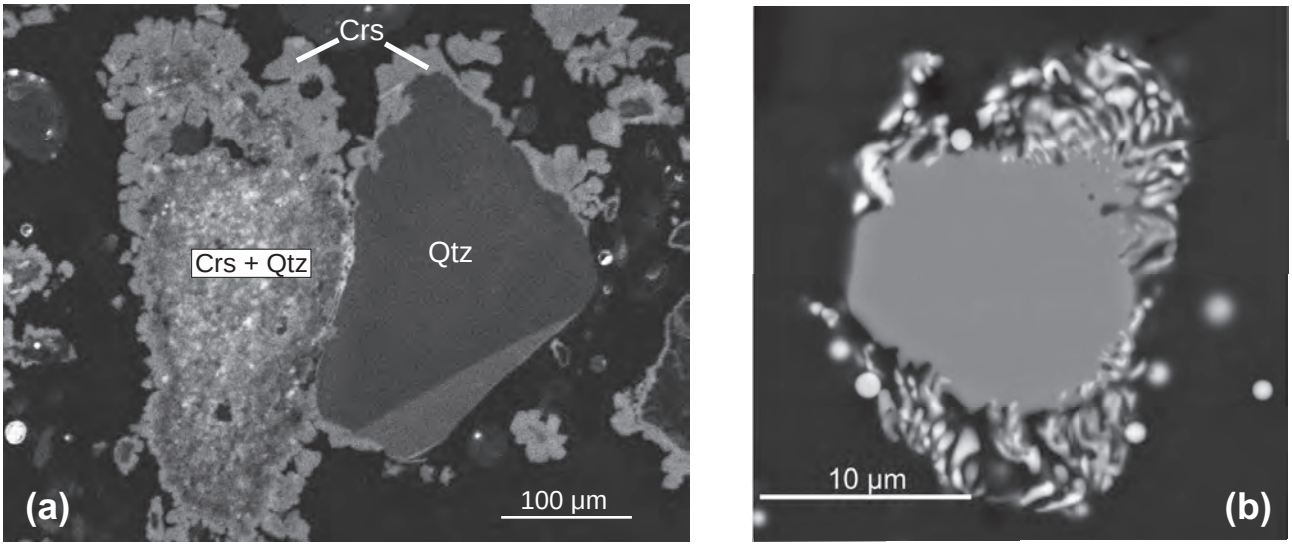

Fig. 8a – Cathodoluminescence image of cristobalite rims (light grey) around quartz (dark grey), set in glass (black). Sample NY13; **b** – Minute baddeleyite grains (white) along the lower and upper tips of a zircon crystal. Glass contains minute spherules of Fe metal. Back-scattered electron (BSE) image.

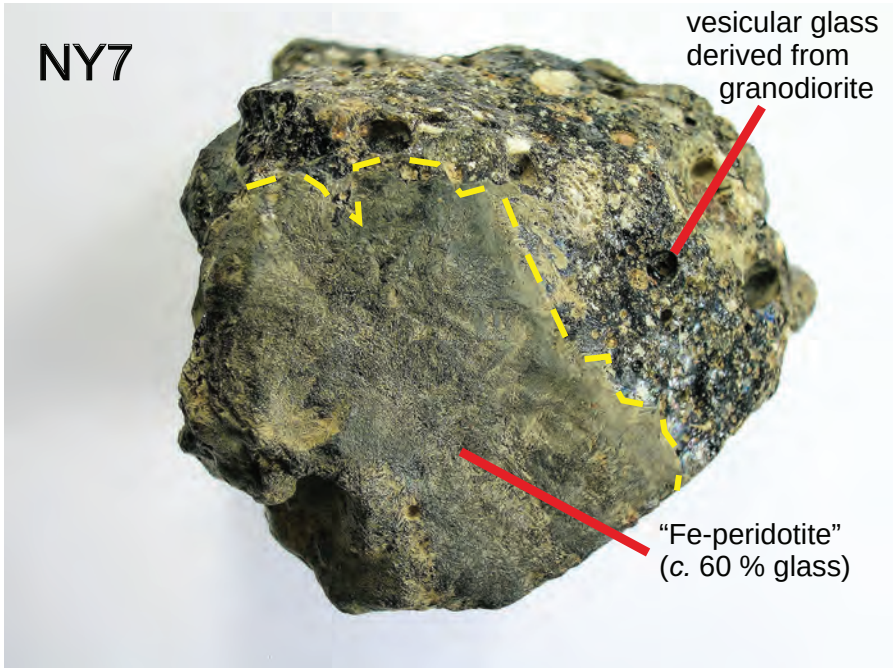

Fig. 9 Three-cm long enclave of Fe-peridotite in vesiculated glass of granodiorite composition.

iron as FeO (mol. %) 67.4 olivine (95.3 % fayalite), 15.6 anorthite, 6.1 nepheline, 4.6 leucite, 1.0 apatite, 0.8 corundum and 0.7 ilmenite.

The analysis of "Fe-peridotite" enclave is included in Tab. 1, column 4. Most unusual is the high whole-rock FeO/MnO ratio of 277, as well as the mg# value [molar 100 × Mg/(Mg + Fe)] of 8.3, suggesting a specific origin of the rock. Interestingly, the extreme FeO/MnO ratio of "Fe-peridotite" accounts for a contamination signature in the local glasses: NY7 (n = 53) has FeO/MnO = 70.8 and NY10 (n = 18) has FeO/MnO = 90.8, i.e. both values are significantly different from the ordinary terrestrial ratio near 58 (Wänke et al. 1988). Admittedly, the original mineralogical composition of the enclave prior to its submergence in vesiculated granodioritic glass is uncertain. But it is possible that a terrestrial analogue of a comparable Fe-peridotite is unknown.

4.4. Natural coke/graphite-rich breccia

In the course of search for glass, a 28 mm long fragment of natural "coke" was found (Fig. 11a–f). The coke/graphite-rich breccia, sample NY14, is highly porous, with approximate volume density of 1.2 and porosity probably near 30–40 vol. %. X-ray powder diffraction analysis shows two very broad peaks corresponding to graphite with poor crystallinity and an approximate size of crystallites near 2 nm. Other phases identified

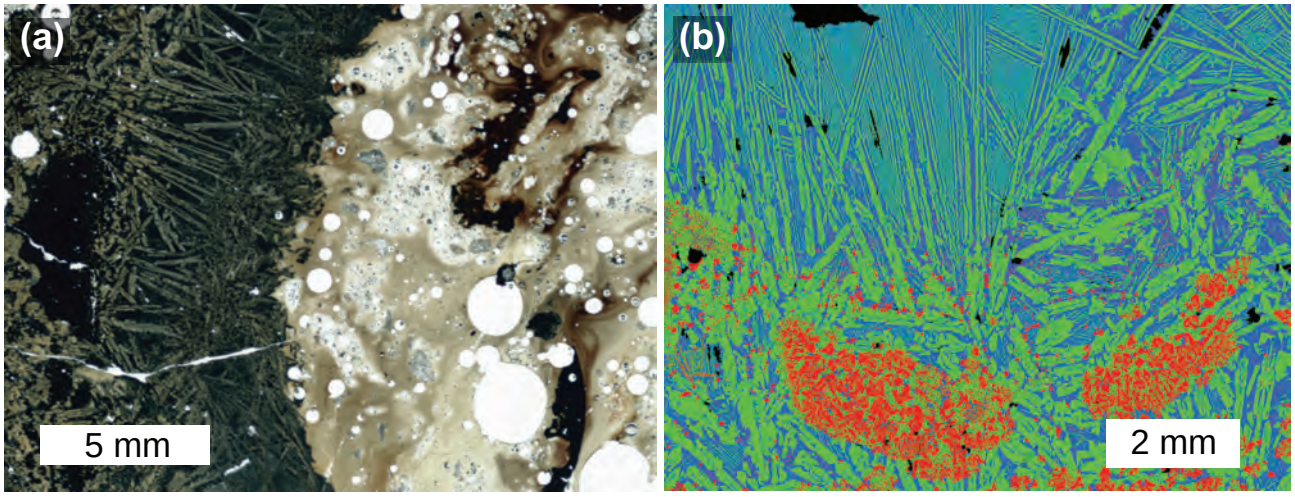

Fig. 10a – Scanner image showing contact of the Fe-rich enclave (dark, left side) with ordinary glass; sample NY7; **b** – A Tescan MIRA phase-map of Fe-peridotite in the same glass sample. Red – magnetite, green – fayalite, blue – glass. image. The whole-rock analysis is in column 4, Tab. 1.

Tab. 1 Major-element contents in several types of glass and inclusions (wt. %)

	Hbl–Bt granodiorite[1]	glass A[2]	glass A*	probable contaminant†	possible contaminant
	Published analyses	NY7 average (n = 53)	NY average (n = 53)	Fe-peridotite inclusion	carbonatite clast
Sample		NY7	NY7	NY7	NY14
SiO_2	63.02	54.32	63.82	32.79	0.68
TiO_2	0.60	0.78	0.92	0.45	
Al_2O_3	15.48	13.11	14.87	9.34	0.16
Cr_2O_3		0.02		0.04	
FeOt	4.42	17.70	6.70	49.24	12.92
MnO	0.10	0.25	0.29	0.16	0.66
CoO		0.02			
NiO		0.01			
MgO	2.87	2.33	2.76	1.35	11.17
CaO	4.31	4.41	4.93	3.36	36.53
Na_2O	3.14	1.28	1.42	1.01	
K_2O	4.03	3.18	3.78	1.80	
P_2O_5	0.24	0.49	0.51	0.44	0.05
SO_3					3.02
F		0.05			
Total		100.00		100.00	65.19

1 – published whole-rock analyses of Hbl–Bt granodiorite (Kozárovice type, n = 6) (Janoušek et al. 2000)
2 – original analyses, glass type A
* – glass type A, corrected for assumed content of 26.18 wt. % of Fe-peridotite (column 4) and recalculated to 100 %.
† – Fe-rich contaminant, Fe-peridotite, (NY7) is important mainly in glass type A

include quartz, cordierite and plagioclase. Carbon isotopic composition with values $\delta^{13}C$ (‰) –23.8 and –24.3 was determined for sample NY14 (unpublished data of the authors).

Electron-microprobe study documents a micro-breccia character of the sample composed dominantly of graphite, glass and mineral fragments. Quartz, K-feldspar, cordierite-related mineral, pyrrhotite and pyrite, Fe° (native iron), minor apatite, TiO_2, magnetite and monazite are estimated to 10–20 vol. % of the sample. Glass clasts exhibit structure similar to flow pattern of molten material (Fig. 11c). Glass dominated by Si and Al (SiO_2 ~50 wt %, Al_2O_3 ~40 wt. %) has composition closely comparable with kaolinite or soil rich in clay minerals (Fig.11d). Most interesting are graphitised fragments of coniferous trees (Fig.11e). Additional interest is in the frequent occurrence of "white graphite" – i.e. material which is white in reflected light, shows a positive relief in polished thin section, indicating hardness higher than that of ordinary graphite, but composed of carbon as ordinary graphite. Pyrrhotite accounts for several vol. % and occurs in several textural modes, including rare fragments with native Fe planar lamellae and spherules that may indicate results of shock deformation (Fig. 12, Mang et al. 2013).

Two carbonatite fragments up to 90 μm long, composed dominantly of Ca-carbonate and ferroan periclase (Fig. 11f), are interesting as a probable source of Ca, Fe, Mg and Mn enrichment detected in parts of the NY13B glass (Fig. 13; Tab. 1). Periclase contains (wt. %) 41.1 FeOt, 53.3 MgO, 2.2 MnO and 0.8 CaO.

4.5. Nature of source rocks and chemical composition of glass

Chemically somewhat variable glass compositions are documented, but the type A predominates (Tab. 1). Numerous EMP analyses (sample NY7, n = 53) provide information on major-element composition of the glass type A (Tab. 1). The analyses indicate similarity to local hornblende–biotite granodiorite (Janoušek et al. 2000; n = 6), but FeOt values of 10 to 13 wt. % exceed those in the granodiorite. As a hypothesis, it was assumed that FeOt contents exceeding 4.0 wt. % (value similar to the granodiorite FeOt content) were introduced as a possible contamination. Consequently, "surplus" FeOt above 4 wt. % and corresponding quantities of other major elements were deducted and the resulting values recalculated to 100 wt. %. Table 1 compares the corrected glass composition with the average for granodiorite. The comparison indicates that the predominating material of glass is indeed close to the local Hbl–Bt granodiorite (Tab. 1). The second compositional type of glass is represented by Al–Si-rich patches corresponding to kaolinite or clay-rich soil, with Al_2O_3 content up to 51.6 wt. %.

The diagrams of CaO vs. major-element oxides (Fig. 13, see ESM 1 for the underlying dataset) show that the type-A glass analyses plot between projection point of granodiorite and the bulk composition of the Fe-peridotite enclave (symbol W in the plot), except for P_2O_5, TiO_2 and MnO. This relation supports the possibility that material similar to Fe-peridotite caused a strong contamination of glass, in particular by iron and siderophile elements.


a

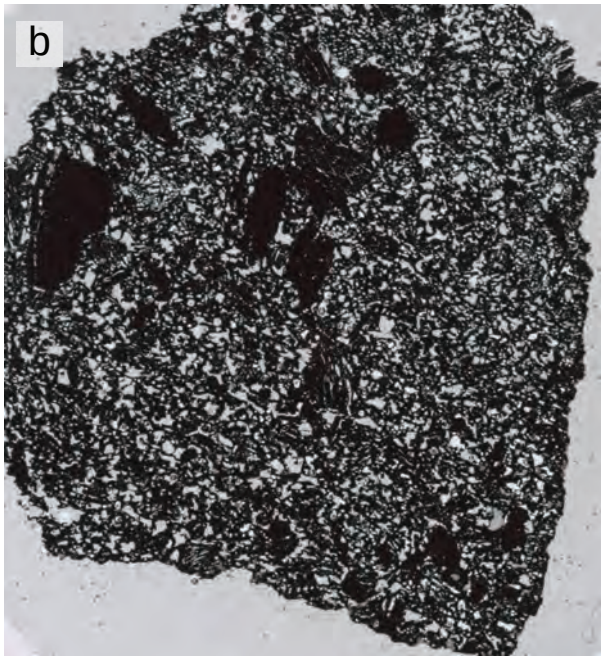
b

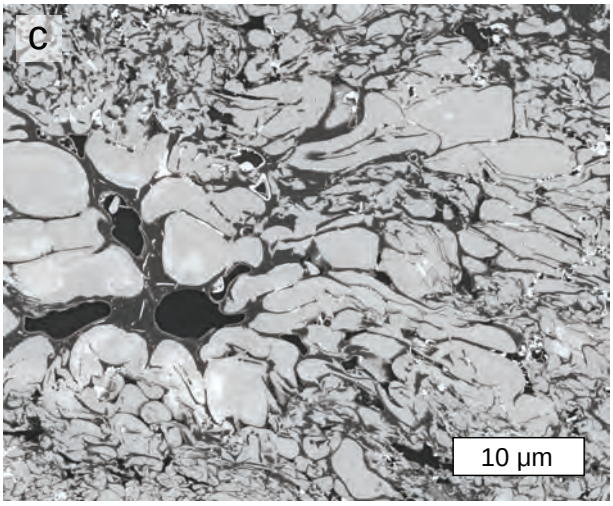
c
10 µm

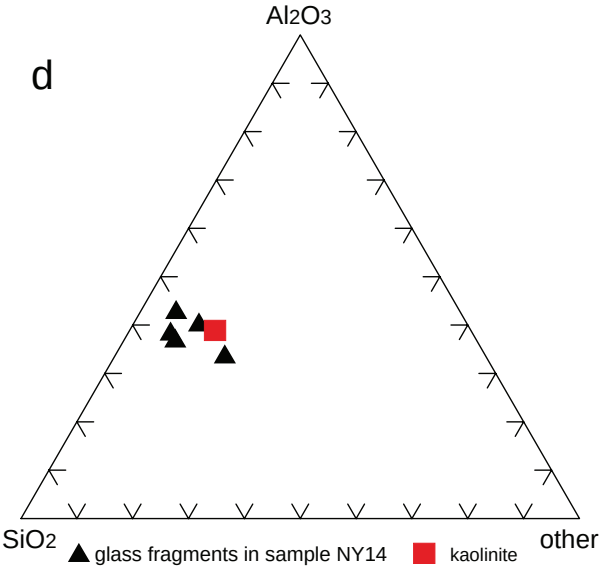
d
Al2O3
SiO2
other
glass fragments in sample NY14
kaolinite

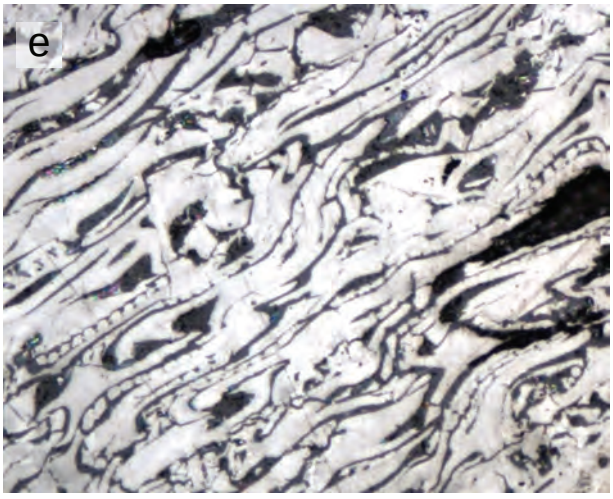
e

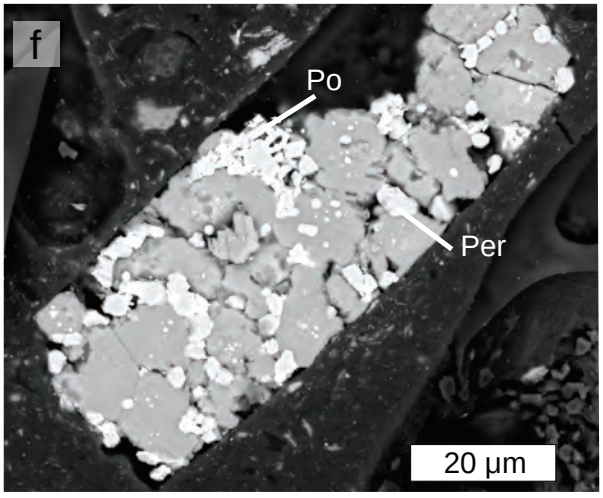
f
Po
Per
20 µm

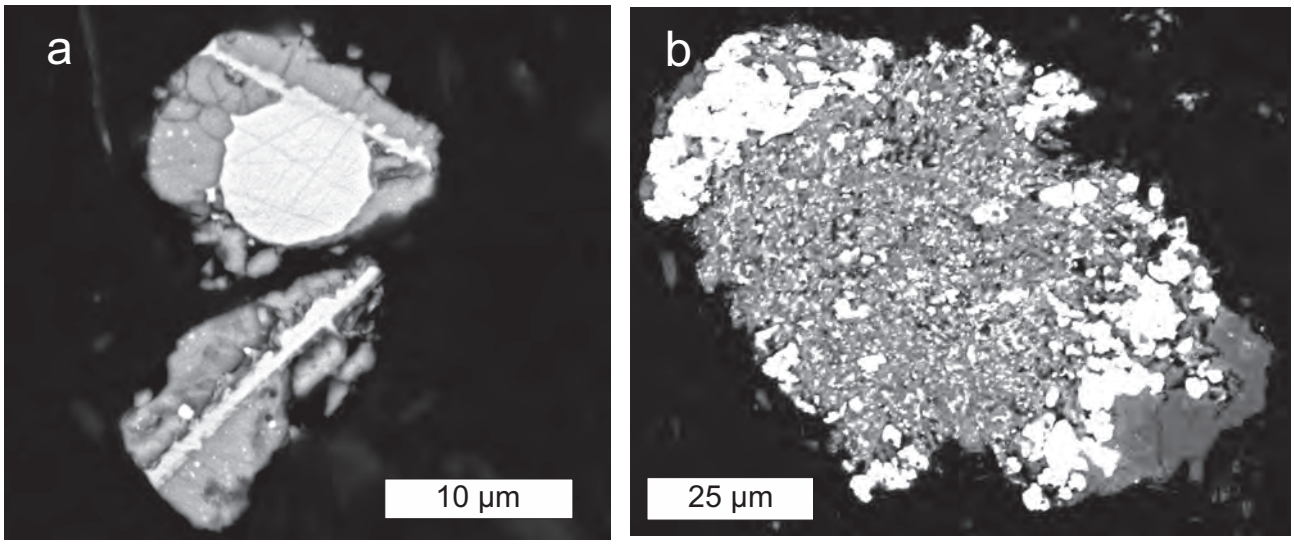

Fig. 12a – Pyrrhotite (medium grey) with lamellae and a spherule of a native iron. Fragments in sample NY14; **b** – Pyrrhotite (white) in intergrowth with glass and other phases. Fragment in sample NY14. Back-scattered electron (BSE) image.

4.5.1. Trace elements, including siderophile ones, and Re–Os isotopic compositions

The trace-element patterns of analyzed glass NY7 mostly mirror those of the surrounding Kozárovice granodiorites (Fig. 16a) (Janoušek and Žák 2015). Nevertheless, LREE concentrations in the glass are systematically lower (La_N/Yb_N = 8.6), compared to the Kozárovice granodiorites (La_N/Yb_N = 10.1–15.3). The relative decline in LREE in glass NY7 is interpreted as being due to a significant admixture of the Fe-rich contaminant (see "Fe-peridotite" inclusion noted above).

The Primitive-mantle normalized (McDonough and Sun 1995) trace-element patterns for glasses show a shape generally similar to the Kozárovice granodiorite; the main difference being more pronounced negative Sr and Ti anomalies in the former (Fig. 14a). Additionally, the glass also contains systematically lower contents of incompatible elements, in particular large-ion lithophile elements (LILE) such as Cs, Rb, Ba, Th and U.

Determined concentrations of highly siderophile (Os, Ir, Ru, Pt, Pd, Re) elements are very low and always below of estimate for the Upper Continental Crust (UCC – Peucker-Ehrenbrink and Jahn, 2001; Fig. 14b). However, the contents of moderately siderophile elements (Cr, Co, Ni) do not differ much (Fig. 14b).

Chromium and Co contents overlap with those determined for the Kozárovice granodiorite, while Ni content of the glass NY7 is only slightly higher (60 ppm vs. <20 to 40 ppm; Tab. 2). Similarly, the measured radiogenic $^{187}Os/^{188}Os$ ratio of 1.04 (Tab. 3) is close to the UCC estimate (~1.4; Peucker-Ehrenbrink and Jahn 2001).

4.5.2. Iron spherules

In sample NY10 metallic Fe spherules several micrometres across contain Ni below the detection limit of the EMP but another iron spherule contains 1.07 wt. % NiO and adjacent magnetite 0.15 wt. % NiO. This observation shows that a minor/moderate Ni- enrichment is locally present. Iron spherules slightly enriched in Ni and Co are documented also in other glass samples. Sample NY13 contains several Fe spherules with phosphorus enriched to 1–8 wt. %. One spherule contains c. 16 wt. % P and corresponds thus to schreibersite, Fe_3P. With reference to trace-element abundances in the glass NY7 (Tab. 2), it is suggested that locally elevated Ni, Co and P contents can be explained as resulting from affinity of these elements to iron.

5. Discussion

5.1. Possible impact origin of the Zalužany circular structure?

With regard to the probable middle Pleistocene age of the study glass (unpublished Ar–Ar data of the authors), there

⇦

Fig. 11a – Fragment of graphite-rich breccia, 28 mm in size; sample NY14; **b** – Scanner image of a thin section of the graphite-rich breccia. Solid black particles are interpreted as graphitised wood fragments. Rock plate is 17 mm wide; **c** – Structure of Si–Al-rich glass with flow pattern similar to that of molten material. A BSE detail from fragment in sample NY14; **d** – Ternary diagram showing compositional similarity of Al–Si-rich glass in sample NY14 to kaolinite. Kaolinite analysis is from *http://www.handbookofmineralogy.org/pdfs/kaolinite.pdf*; **e** – Probable relict structures of deformed conifer wood in graphitized fragment; sample NY14; reflected light microscopy; **f** – Secondary Electron Microscopy (SEM) image of carbonatite clast in the graphite-rich breccia. Carbonate – medium grey, periclase–wustite zoned crystals – Per, pyrrhotite – Po.

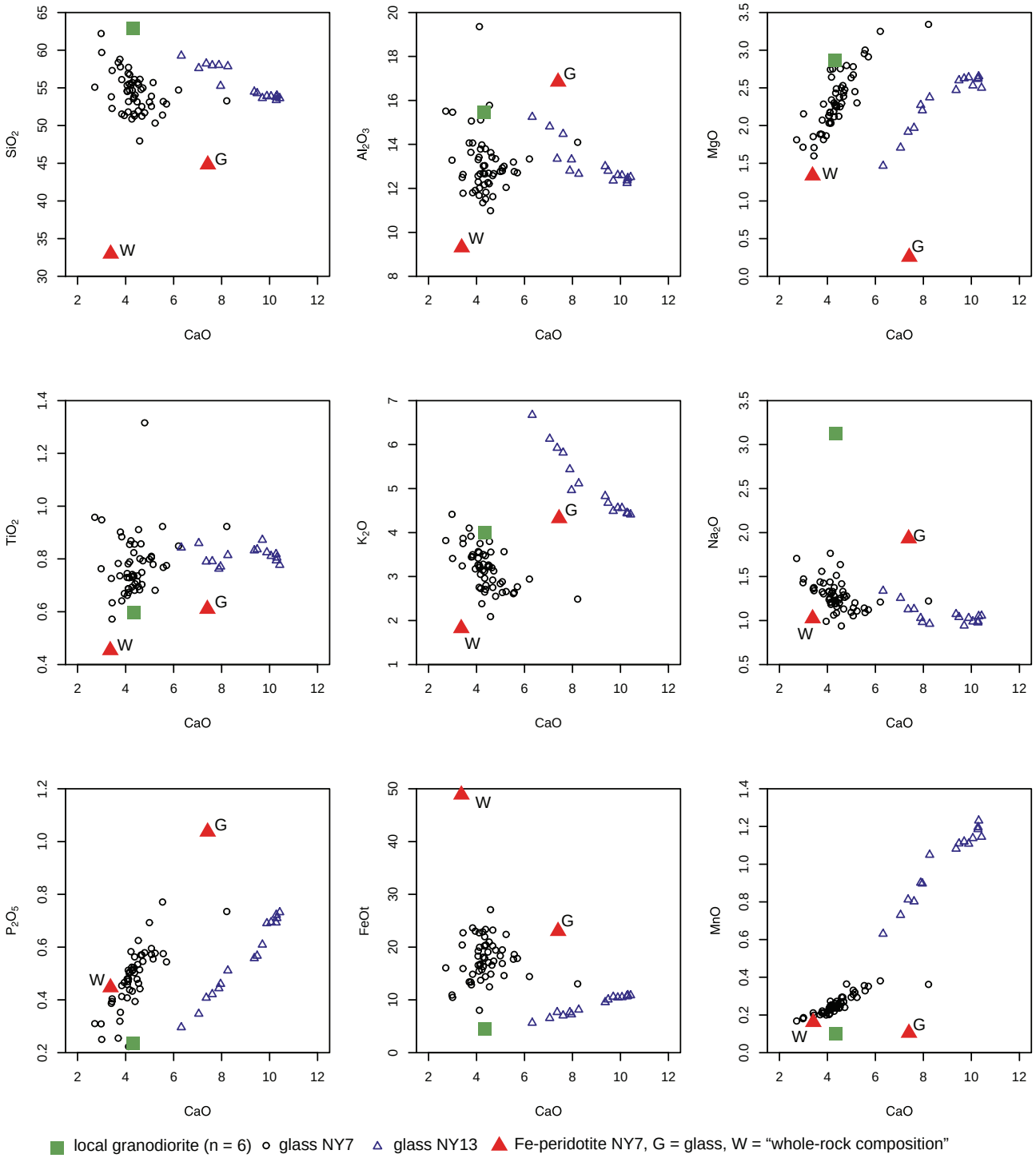

Fig. 13 Impact glass compositions in diagrams of CaO vs. other major-element oxides (wt. %). Glass type A (NY7, n = 53) and type B (sample NY13, n = 16) compositions are compared with the local granodiorite and a Fe-peridotite inclusion (49.2 wt. % FeO) in glass sample NY7 (W = "whole-rock composition"; G = glass composition of Fe-peridotite inclusion). Note that for SiO_2, Al_2O_3, FeO, MgO, K_2O, Na_2O, and P_2O_5, projection points for glass type A plot along the tie-line granodiorite–W (bulk composition of the Fe-peridotite inclusion).

is no indication of Quaternary volcanism in central Bohemia, which would permit to interpret the Zalužany circular structure as volcanogenic. Unlike in the Ohře Rift region of western Bohemia (Mrlina et al. 2009), there is also an absence of recent seismicity, no release of upper mantle fluids and the lack of Pleistocene basaltic clasts or pumice in central Bohemia. As an alternative explanation (working hypothesis) we will discuss a possible origin by impact.

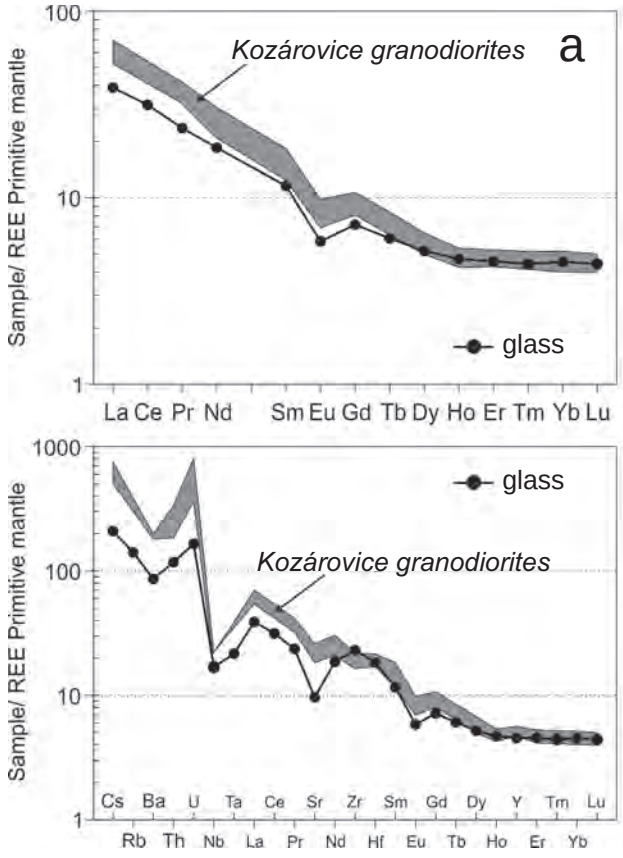

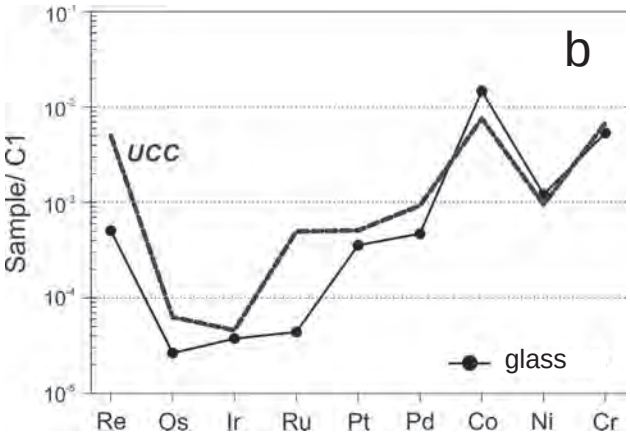

Fig. 14a Comparison of trace elements in Kozárovice granodiorite (Janoušek et al. 2000, 2010) and in glass sample NY7, spiderplots normalized by Primitive Mantle composition of McDonough and Sun (1995); **b** – C1 chondrite-normalized (Jochum 1996; Anders and Grevesse 1989) abundances of siderophile elements in glass NY7 compared with the average Upper Continental Crust (UCC) data (Peucker-Ehrenbrink and Jahn 2001).

The experience of impact structure studies (French and Koeberl 2010) shows the importance of identification of planar deformation features (PDF) in quartz and of shatter cones as evidence of shock wave operation in production of a given circular structure. As a matter of fact, both PDF and shatter cones are absent in many small impact structures *c.* 100–200 m diameter, which however qualify as meteorite craters, owing to finds of fragments of the meteorite impactor. The Zalužany circular structure (d = 500 m) is not dramatically larger. If we accept the impact hypothesis as a possible explanation for the Zalužany structure origin, consider the presence of two gravity lows and the shape of the main gravity anomaly, the impactor would have had a low-angle trajectory, most likely from SE to NW. Reliable and well-studied examples for such trajectories are absent in the literature.

The Hejný pond shows a prominent bilateral symmetry (Fig. 1). The pivotal accumulation of debris and the morphological indication of backward movement of debris shown by morphology on NW side of the

Tab. 2 Trace-element composition of glass sample NY7 (ppm)

Sample	NY7		NY7
Li	30	La	25
Sc	11	Ce	53
V	77	Pr	6.0
Cr	72	Nd	23
Co	33	Sm	4.7
Ni	60	Eu	0.88
Cu	58	Gd	3.9
Zn	8.0	Tb	0.60
Rb	84	Dy	3.5
Sr	192	Ho	0.69
Y	19	Er	2.0
Zr	243	Tm	0.30
Nb	11	Yb	2.0
Cs	4.4	Lu	0.29
Ba	569	Hf	5.2
		Ta	0.8
		Pb	3.8
		Th	9.4
		U	3.3

Tab. 3 Contents of platinum-group elements (ppb) and Re–Os isotopic composition of the glass sample NY7

Sample	NY7
Re	0.020
Os	0.013
Ir	0.018
Ru	0.026
Pt	0.35
Pd	0.26
$^{187}Re/^{188}Os$	8.3
$^{187}Os/^{188}Os$	1.04

Hejný pond bank point to a significant subhorizontal vector in debris movements accompanying the crater excavation. Information on oblique impacts (Gault and Wedekind 1978; Pierazzo and Melosh 2000) indicates that for an oblique impact with trajectory angle of 15° the volume of melt drops by 90 % as compared to the vertical trajectory and deformation effects are also reduced. The relative rarity of glass would support the role of oblique trajectory as associated with the reduced extent of melting.

5.2. Gravity

The gravity anomaly coincides with the southwestern part of the pond (Fig. 3); however, we cannot either claim, or exclude that it would extend over most of the pond in case we could perform the measurements over the whole pond area. The small prolongation to the south can be explained by alluvium accumulation in the drainage zone (small valley with a brook). The low amplitude of the gravity anomaly (–0.35 mGal) would support oblique low-angle impact trajectory with significantly limited rock deformation expressed by decreased bulk density of the rock massif.

The main gravity anomaly is elongated SE–NW and 0.5 km to the NW it is accompanied by another smaller negative anomaly. This situation could suggest importance of a SE–NW vector in shaping the circular structure as a supportive factor for the impact hypothesis. The studied glass samples were found at the W–NW side of the gravity anomaly, i.e. in the assumed direction of the material transport. Owing to the absence of gravity data in the main part of the pond with water, the relation between surface morphology and gravity field is not sufficiently clarified.

5.3. Properties of glass

The glass composition mimics the composition of local amphibole–biotite granodiorite (Tab. 1, Fig. 13). Glass contains contamination components, corresponding to "Fe-peridotite" fragments in glass type A (Tab. 1), and kaolin-rich soil. Three individual glass batches at somewhat different locations with the same or similar ("Fe-peridotite") contamination can be explained by production of all glass in a single event. The "Fe-peridotite" component contamination is strongly demonstrated by the high FeO/MnO ratio in NY7 glass (n = 53) FeO/MnO = 70.8; NY10 glass (n = 18) FeO/MnO = 90.8. The probable Middle Pleistocene age of glass directly excludes the role of man in its production.

Moreover, the temperature of formation above 1673 ± 10 °C is proved by local zircon dissociation to ZrO_2 + SiO_2 (Kaiser et al. 2008). The given temperature of ZrO_2 formation relates to pressure of 1 atm. However, it can be produced also at high-pressure events (*c.* 53–94 GPa) and temperatures in the order of thousands degrees. As baddeleyite is not stable above 1 200 °C (Kusaba et al. 1985; Kaiser et al. 2008) it apparently reverted from a higher-symmetry polymorph of ZrO_2. Quartz melting to lechatelierite at > 2 000 °C is assumed on the basis of lechatelierite formation in tektites (Macris et al. 2014). Cooling of SiO_2 melt to lechatelierite in Zalužany glass is directly proven by vesicular structures, in which vesicles formed in the process of SiO_2 melt boiling (Fig. 6). Much of lechatelierite crystallized in turn to cristobalite. In any case, the high-temperature indications are not compatible with a scenario of glass production in fires set by the Neanderthals.

Exotic rock inclusions in glass (columns 4 and 5 in Tab. 1) are not only of interest as such, but are important as their chemistry corresponds to the likely contaminants of the glass. This situation comes near to the case of impact glasses with contamination by respective meteoritic impactors. It remains for a future study of the inclusions in a laboratory equipped for a geochemical and isotope study on microscopic scale, whether an extra-terrestrial origin can be established. The alleged exotic rock character is associated with 1) "Fe-peridotite" composition containing 49 wt. % FeOt (Tab. 1). Rocks of this composition are unknown in central Bohemia. 2) Periclase carbonatite is a unique rock type known globally only from the Oka carbonatite complex in Quebec, Canada (Treiman and Essene 1984). Central Bohemia is dominated by Variscan plutonic granitoids and some Neoproterozoic to lower Paleozoic volcanosedimentary rocks. No carbonatites are known in this region.

6. Conclusions

The main features of the Zalužany circular structure are shown in topographic and gravity maps. The present detailed gravity survey revealed the existence of a negative gravity anomaly oriented SE–NW at the south-western rim of the pond (i.e. the area that we could not survey). Considering the findings of glass and breccia at the NW side of the gravity low we may suggest a working hypothesis of oblique low-angle SE to NW impact with limited rock deformation (minor decrease in rock massif bulk density). The low amplitude of the gravity anomaly then corresponds with such assumption. Moreover, it is not easy to find another explanation for the gravity low in the more or less homogeneous granodiorite massif.

The chemical composition of glass, after correction for the contamination components, compares closely with the putative target rock – the Kozárovice hornblende–biotite granodiorite – that exhibits only limited compositional

variation. The evidence is strengthened by identification of additional lithology – Al-rich soil or kaolinite-rich clay as a part of the local weathering crust. Glass contains numerous, fine-grained pseudomorphs after original quartz fragments, composed of quartz and cristobalite. It is important that BSE images show numerous vesicles in the aggregates. These structures are diagnostic of previous history of quartz melting and SiO_2 melt boiling, solidified as lechatelierite and transformed in turn to cristobalite. Locally we diagnosed ballen-structures in cristobalite – they are considered as impact melting indicator in literature, similarly to zircon grains in glass altered to baddeleyite. The exotic iron-rich enclave of "Fe-peridotite" (49.2 wt. % FeOt), documented in one of glass samples, corresponds to the contamination component in glass type A.

On the other hand, important indicators supporting the hypothesis of the impact origin of the Zalužany structure are missing at present: presence of PGE and Ni enrichment in (impact) glass, planar deformation features in local rocks and shatter cones exhibiting a typical morphology.

The first criterion – highly siderophile element (e.g., PGE) enrichment – would be missing in case of an achondrite or planetary projectile. The possible oblique impact would reduce the deformation in the local rocks. Also the advanced degree of Pleistocene erosion around the Zalužany structure could have removed much of the impact morphological features.

To sum up, even though we have focused in the current paper on listing number of geophysical and geochemical arguments in favour of the impact hypothesis, there are still open questions to be resolved prior proving such an origin of the Zalužany structure. In particular, a borehole located in a gravimetry minimum would be a fundamental step toward recognition of sub-surface geology and possibly to sampling highly deformed breccias affected by shock-deformation.

Acknowledgements. Our thanks go to Lukáš Ackerman, who worked out on highly siderophile element systematics and trace-element contents in impact glass sample NY7, but due to his research stay in USA, he decided to break cooperation on the Zalužany topic. Nevertheless, L. Ackerman agreed that we use his data in the current presentation. Work of the first author (S.V.) was supported by Project No. 321350 of the Czech Geological Survey. We appreciate field work of Václav Polák and Michal Seidl who performed geodetic measurements as support for the gravity survey. We acknowledge numerous comments by Tomáš Kohout and other reviewer that helped us to improve the manuscript. We certainly wish to thank the handling editor, Roman Skála, and editor-in-chief Vojtěch Janoušek for general notes to the manuscript as well as for numerous specific comments to its geochemical part.

Electronic supplementary material. Supplementary table with chemical compositions of glasses NY7S and NY13S, a 'Fe-peridotite' NY7 and average Kozárovice granodiorite (wt. %) is available online at the Journal web site (*http://dx.doi.org/10.3190/jgeosci.281*).

References

Anders E, Grevesse N (1989) Abundances of the elements – meteoritic and solar. Geochim Cosmochim Acta 53: 197–214

Bates JB (1972) Raman spectra of α and β cristobalite. J Chem Phys 57: 4042–4047

Birck JL, Barman MR, Capmas F (1991) Re–Os isotopic measurements at the femtomole level in natural samples. Geostand Newsl 20: 19–27

Cohen AS, Waters FG (1996) Separation of osmium from geological materials by solvent extraction for analysis by thermal ionisation mass spectrometry. Anal Chim Acta 332: 269–275

Creaser RA, Papanastassiou DA, Wasserburg GJ (1991) Negative thermal ion mass spectrometry of osmium, rhenium, and iridium. Geochim Cosmochim Acta 55: 397–401

Ferrière L, Koeberl C, Reimold WU (2009) Characterisation of ballen quartz and cristobalite in impact breccias: new observations and constraints on ballen formation. Eur J Mineral 21: 203–217

French BM, Koeberl C (2010) The convincing identification of terrestrial meteorite impact structures: what works, what doesn't and why. Earth Sci Rev 98: 123–170

Gault DE, Wedekind JA (1978) Experimental studies of oblique impact. In: Proceedings of the 9th Lunar and Planetary Science Conference, Houston, Tex., March 13–17, 1978, Volume 3. Pergamon Press, New York, pp 843–3875

Hutchison CS (1974) Laboratory Handbook of Petrographic Techniques. John Wiley & Sons, New York, pp 1–527

Janoušek V, Žák J (2015) Kozárovice – a high-K calc-alkaline intrusion of the Blatná Suite, magma mixing phenomena. In: Janoušek V, Žák J (eds) Eurogranites 2015. Variscan Plutons of the Bohemian Massif. Post-conference field trip following the 26th IUGS General Assembly in Prague. Czech Geological Survey, Prague, pp 48–55

Janoušek V, Bowes DR, Braithwaite CJR, Rogers G (2000) Microstructural and mineralogical evidence for limited involvement of magma mixing in the petrogenesis of a Hercynian high-K calc-alkaline intrusion: the Kozárovice granodiorite, Central Bohemian Pluton,

Czech Republic. Trans Roy Soc Edinb, Earth Sci 91: 15–26

Janoušek V, Farrow CM, Erban V (2006) Interpretation of whole-rock geochemical data in igneous geochemistry: introducing Geochemical Data Toolkit (GCDkit). J Petrol 47: 1255–1259

Janoušek V, Wiegand B, Žák J (2010) Dating the onset of Variscan crustal exhumation in the core of the Bohemian Massif: new U–Pb single zircon ages from the high-K calc-alkaline granodiorites of the Blatná suite, Central Bohemian Plutonic Complex. J Geol Soc, London 167: 347–360

Jochum KP (1996) Rhodium and other platinum-group elements in carbonaceous chondrites. Geochim Cosmochim Acta 60: 3353–3357

Jonášová Š, Ackerman L, Žák K, Skála R, Ďurišová J, Deutsch A, Magna T (2016) Geochemistry of impact glasses and target rocks from the Zhamanshin impact structure, Kazakhstan: implications for mixing of target and impactor matter. Geochim Cosmochim Acta 190: 239–264

Kaiser A, Lobert M, Telle R (2008) Thermal stability of zircon ($ZrSiO_4$). J Eur Ceram Soc 28: 2199–2211

Kusaba K, Syono Y, Kikuchi M, Fukuoka K (1985) Shock behaviour of zircon. Phase transition to scheelite structure and decomposition. Earth Planet Sci Lett 72: 433–439

Macris CA, Badro J, Asimow PD, Eiler JM, Stolper EM (2014) Seconds after impact: insights from diffusion between lechatelierite and hot glass in tektites and experiments. Meteorit Planet Sci 49: A5–A454

Mang C, Kontny A, Fritz J, Schneider R (2013) Shock experiments up to 30 GPa and their consequences on microstructures and magnetic properties in pyrrhotite. Geochem Geophys Geosyst 14: 63–85

McDonough WF, Sun SS (1995) The composition of the Earth. Chem Geol 120: 223–253

Mrlina J (2016) Near-surface characterization for seismic exploration based on gravity and resistivity data. Proceedings of the Conference GEO 2016, Bahrain. Online Journal for E&P Geoscientists, AAPG Datapages Inc., Paper #41892, pp 1–11

Mrlina J, Kämpf H, Geissler WH, van den Boogart P (2007) Assumed Quaternary maar structure at the Czech/German boundary between Mýtina and Neualbenreuth (western Eger Rift, Central Europe): geophysical, petrochemical and geochronological indications. Z geol Wiss 35: 213–230

Mrlina J, Kämpf H, Kroner C, Mingram J, Stebich M, Geissler WH, Kallmeyer J, Matthes H, Seidl M (2009) Discovery of the first Quaternary maar in the Bohemian Massif, Central Europe, based on combined geophysical and geological surveys. J Volcanol Geotherm Res 182: 97–112

Peucker-Ehrenbrink B, Jahn B-M (2001) Rhenium–osmium isotope systematics and platinum group element concentrations: loess and the upper continental crust. Geochem Geophys Geosyst 2: 1061. DOI 10.1029/2001GC000172

Pierazzo E, Melosh HJ (2000) Melt production in oblique impacts. Icarus 145: 252–261

Pouchou JL, Pichoir F (1985) "PAP" (ϕ–ρ–Z) procedure for improved quantitative microanalysis. In: Armstrong JT (ed) Microbeam Analysis. San Francisco Press, San Francisco, 104–106

Reimold WU, Koeberl C, Gibson RL, Dressler BO (2005) Economic mineral deposits in impact structures: a review. In: Koeberl C, Henkel H (eds) Impact Tectonics. Impact Studies. Springer, Berlin, Heidelberg, pp 479–552

Rohrmüller J, Kämpf H, Geiss E, Grossmann J, Grun I, Mingram J, Mrlina J, Plessen B, Stebich M, Veress C, Wendt A, Nowaczyk N (2018) Reconnaissance study of an inferred Quaternary maar structure in the western part of the Bohemian Massif near Neualbenreuth, NE-Bavaria (Germany). Int J Earth Sci (Geol Rundsch) 107: 1381–1405

Shirey S B, Walker RJ (1995) Carius tube digestion for low-blank rhenium–osmium analyses. Anal Chim Acta 67: 2136–2141

Treiman AH, Essene EJ (1984) A periclase–dolomite–calcite carbonatite from the Oka Complex, Quebec, and its calculated volatile composition. Contrib Mineral Petrol 85: 149–157

Völkening J, Walczyk T, Heumann KG (1991) Osmium isotope ratio determinations by negative thermal ionization mass spectrometry. Int J Mass Spectrom Ion Processes 105: 147–159

Wänke H, Dreibus G (1984) Mantle chemistry and accretion history of the Earth. In: Kröner A, Hanson G, Goodwin A (eds) Archaean Geochemistry. Springer, Berlin, pp l–24